Luminescence from the 3 P 2 State of Tm 3+

ARTICLE *in* THE JOURNAL OF PHYSICAL CHEMISTRY B · APRIL 2002

Impact Factor: 3.3 · DOI: 10.1021/jp0138680

Luminescence from the $^3P_2$ State of Tm^{3+}

Peter A. Tanner,*,† Chris S. K. Mak,† Wai Ming Kwok,‡ David L. Phillips,‡ and Marie-France Joubert§

Department of Biology and Chemistry, City University of Hong Kong, Tat Chee Avenue, Kowloon, Hong Kong SAR, People's Republic of China, Department of Chemistry, The University of Hong Kong, Pokfulam Road, Hong Kong, People's Republic of China, and Laboratoire de Physico-Chimie des Matériaux Luminescents, Université Claude-Bernard Lyon-1, UMR 5620 du CNRS, Bâtiment A. Kastler, 69622 Villeurbanne Cedex, France

Received: October 18, 2001; In Final Form: February 6, 2002

Using various ultraviolet laser excitation lines between 199.8 nm (50 034 cm^{-1}) and 266 nm (37 583 cm^{-1}), emission transitions have been observed and assigned for the first time from the $^3P_2$ term of Tm^{3+}, located near 37 500 cm^{-1}. The most intense transitions are to the terminal $^3H_6$ and $^3F_4$ states, and are almost entirely vibronic in character for Tm^{3+} in elpasolite cubic lattices. In other systems, these transitions may find application in ultraviolet lasers. The interpretation of the $^3P_2 \rightarrow {}^3H_4$ emission transition in $Cs_2NaTmCl_6$ reveals electron−phonon coupling phenomena analogous to that in the $^3H_6$ ground state, and which provides the explanation for the enormous deviation between the experimental and calculated energy of the $^3H_4$ Γ_4 level. We also report the quantum cutting of blue to infrared radiation in $Cs_2LiTmCl_6$ and the upconversion from $^1D_2$ to $^3P_2$ in $Cs_2NaTmCl_6$.

Introduction

Recently, Dieke's diagram has been extended into the vacuum ultraviolet for several lanthanide ions from the excitation spectra using synchrotron radiation.[1] We are investigating the ultraviolet emission spectra of lanthanide ions from previously uncharacterized levels,[2] using H_2-shifted frequency-tripled Nd:YAG excitation. Herein we report extensive luminescence from the $^3P_2$ term of Tm^{3+}. Although this term has been previously located from absorption measurements,[3] we are unaware of any previous report of its luminescence transitions.

We also report the upconversion from the Tm^{3+} $^1D_2$ energy level to the $^3P_2$ level. Upconversion results when a single ion in a crystalline lattice attains a higher energy level than the energy of incident photons, by way of processes such as excited-state absorption, energy transfer, or two-photon excitation. In the case reported, the $^3P_2$ energy is some 16 000 cm^{-1} higher than the incident photon energy. A downconversion process has also been found, and is reported for $Cs_2LiTmCl_6$. Here, the *quantum cutting* of an incident blue photon (of energy ca. 21 000 cm^{-1}) results in the emission of several infrared photons.

Various studies of the optical spectra of Tm^{3+} in different host lattices have been cited by Hölsä et al.[4] Lasing under infrared pumping has been investigated for Tm^{3+} and Tm^{3+}−Yb^{3+} codoped systems.[5] For Tm^{3+} diluted in elpasolite host lattices, blue luminescence has previously been reported from the $^1G_4$ term in dilute $Cs_2NaGdCl_6$:Tm^{3+} [6,7] and from the $^1D_2$ term in Cs_2NaYCl_6:Tm^{3+}.[8,9] The electronic spectra of Tm^{3+} in elpasolite lattices have been studied extensively,[6,10] and the most recent energy level calculations are given in ref 11.

TABLE 1: Vibronic Displacement Energies from Zero Phonon Lines in the Electronic Spectra of $Cs_2NaTmCl_6$ and $Cs_2LiTmCl_6$[a]

unit cell group mode[14]	moiety mode	displacement energy (cm^{-1}) from electronic origin and typical relative intensity		
		$Cs_2NaTmCl_6$	$Cs_2LiTmCl_6$	Cs_2LiYCl_6:Tm
S_5 τ_{2g} Cs^+ lattice	-	47m	462, 53m	38,44
S_6 τ_{1u} Ln-Cl str.	ν_3	244m, 257s, 285mw	226m, 250s, 283mw, 320vw	262
S_7 τ_{1u} Cl-Ln-Cl b.	ν_4	113s, 132w	109m, 119s, 140w	99s, 112vw
S_8 τ_{1u} M-Cl str.	-	182mw	207m	197w
S_9 τ_{1u} Cs^+ transl.	-	55 mw	66m, 73mw	58
S_{10} τ_{2u} Cl-Ln-Cl b.	ν_6	79w, 86s	94m, 99s, 104w	68s,79sh
ZB acoustic		36w		

[a] transl., translation; str., stretch; b., bend; ZB, zone boundary. The relative intensities are an approximate average guide : m, medium; s, strong; w, weak; M = Na, Li.

Experimental Section

Cs_2MTmCl_6 (M = Li, Na), Cs_2LiYCl_6:Tm^{3+}, and $Cs_2NaGdCl_6$:Tm^{3+} were prepared as powders in sealed quartz tubes using Morss Method E,[12] as described previously.[6] Dry hydrogen chloride gas was passed over these powders at 420 °C for 2 days, before passage through a Bridgman furnace at 800−850 °C. We were unable to synthesize pure crystals by the ammonium chloride method.[13] The Tm_2O_3 and Y_2O_3 starting materials were of 99.9% (Strem Chemicals) and 99.999% (Berkshire Ores) purity, respectively. Inductively coupled plasma−atomic emission spectroscopic analysis of the Tm_2O_3 starting material showed the presence of 2.8 ppm Ce, 21 ppm Pr, and 0.3 ppm Nd. Crystals were mounted in an Oxford Instruments closed-cycle cooler cryostat for the emission spectra recorded at Hong Kong University at 10 K, using a resolution

* Corresponding author. Fax: (852) 2788 7406. E-mail: bhtan@cityu.edu.hk.
† City University of Hong Kong.
‡ The University of Hong Kong.
§ Université Claude-Bernard Lyon-1.

10.1021/jp0138680 CCC: $22.00
Published on Web 00/00/0000 PAGE EST: 5.8

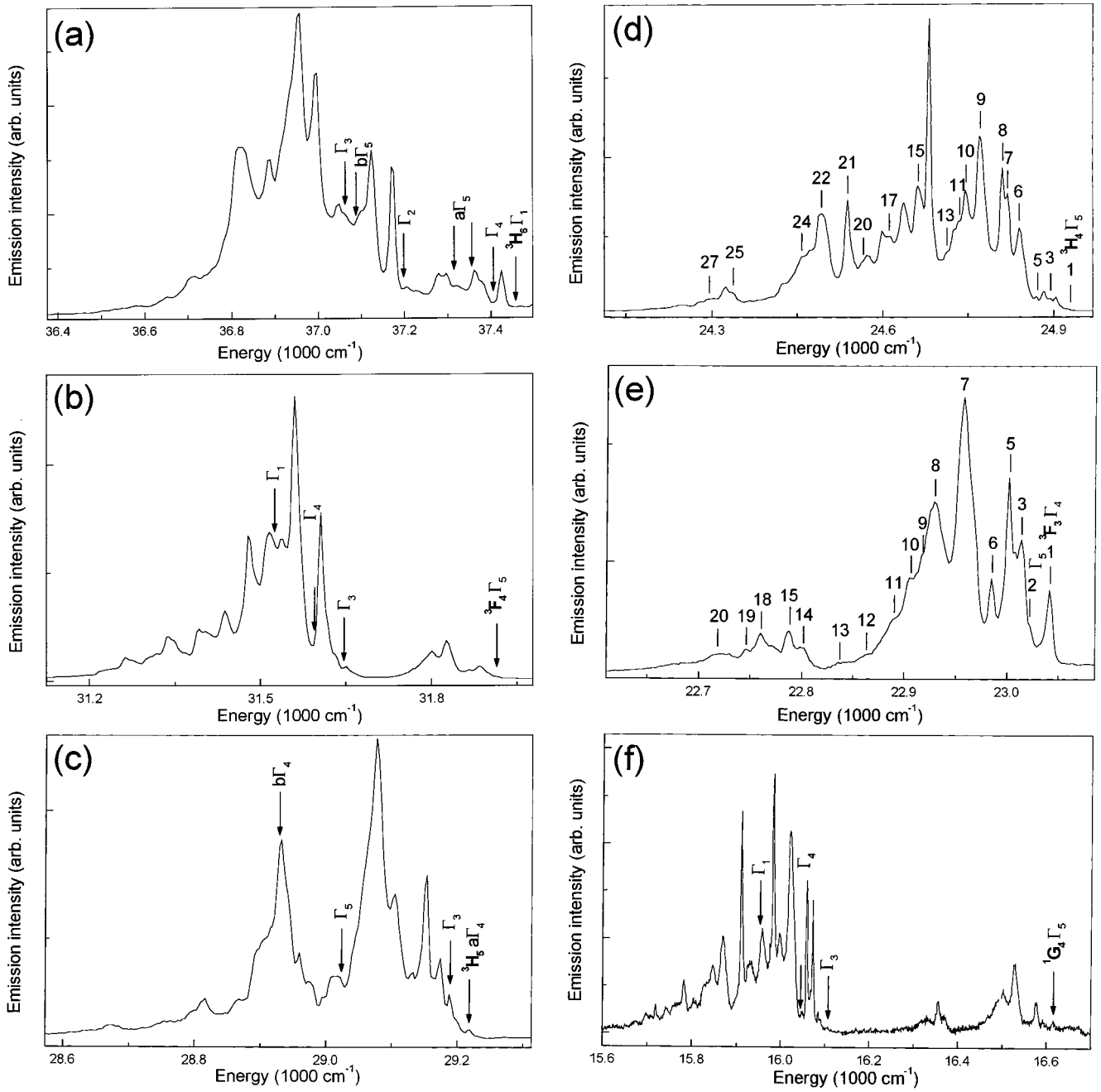

Figure 1. (a)−(f) The 204.2 nm excited 10 K emission spectrum of $Cs_2NaTmCl_6$ between 37 500 and 15 000 cm^{-1}. The upper level is $^3P_2$ Γ_3 in all cases. Refer to Tables 3 and 4 for line assignments of (d) and (e), respectively.

of 0.05 nm (ca. 4 cm^{-1}) from 190 to 800 nm. In these experiments the sample was excited by the anti-Stokes H_2-shifted harmonics of 266 nm radiation from a Nd:YAG pulsed laser, or by the 476.5 nm (20 981 cm^{-1}) line of an argon ion laser. The emission was collected at 90° and passed through an Acton 0.5-m spectrometer, with a liquid-N_2-cooled SDS 9000 charge-coupled device (Photometrics). The emission line energies were converted to vacuum wavenumbers.

Room-temperature spectroscopy of $Cs_2NaTmCl_6$ and $Cs_2NaGdCl_6$:Tm^{3+} was also investigated at the Université Claude Bernard Lyon-1. The luminescence was excited by an excimer laser with variable pulse repetition rate (duration 10 ns, energy 40 mJ at 308 nm), followed by a dye laser. Pulsed radiation at 360.97 nm (27 695 cm^{-1}) was employed for excitation into the $^1D_2$ term of Tm^{3+} and at 467.76 nm (21 373 cm^{-1}) for excitation into $^1G_4$. Luminescence was detected with a Hilger and Watts monochromator (dispersion 0.8 nm mm^{-1}) equipped with an RCA GaAs photomultiplier. The signal was processed with an Ortec photon counting system. The setup was controlled with a PC. Decay times were measured with a Canberra 35+ multichannel analyzer with the maximum resolution 200 ns per channel.

Results and Discussion

Ultraviolet Excitation of $^3P_2$ Emission in $Cs_2NaTmCl_6$. The electronic ground state of the f^{12} ion Tm^{3+} in $Cs_2NaTmCl_6$ is $^3H_6$ Γ_1 (the gerade subscript is omitted throughout).[11] The electronic spectra of this ion in cubic crystals comprise electric quadrupole and/or magnetic dipole allowed zero phonon lines, and extensive vibronic sidebands involving single ungerade phonons and lattice vibrations.[6] The energies and assignments of vibronic structure in the electronic spectra of $Cs_2NaTmCl_6$ are included in Table 1. Two notations are given for the moiety and unit cell group vibrational modes.[14]

TABLE 2: $^3P_2$ Emission Transition Energies and Derived Energy Levels (cm^{-1}) for Tm^{3+} in $Cs_2NaTmCl_6$

SLJ	$\gamma\Gamma$	electronic origin energy from $^3P_2$ emission spectrum	derived terminal state energy	energy in $Cs_2NaTmCl_6$[a]
$^3H_6$	Γ_1	37 460	0	0
	Γ_4	37 404	56	56
	aΓ_5	37 356	104	108
		37 313	147	148
	Γ_2	37 199	261	261
	bΓ_5	37 090	370	370
	Γ_3	37 066	394	394
$^3F_4$	Γ_5	31 914	5 546	5 547
	Γ_3	31 647	5 813	5 814
	Γ_4	31 595	5 865	5 866
	Γ_1	31 523	5 937	5 938
$^3H_5$	aΓ_4	29 221	8 239	8 241
	Γ_3	29 189	8 271	8 270
	Γ_5	29 024	8 436	8 436
	bΓ_4	28 928	8 532	8 532
$^3H_4$	Γ_5	24 924	12 536	12 538
	Γ_3	24 855	12 605	12 607
	Γ_4	24 768	12 692	
		24 620	12 840	12 840
	Γ_1	24 581	12 879	12 882
$^3F_3$	Γ_2	22 993	14 467	
	Γ_4	23 034	14 426	14 431
	Γ_5	23 007	14 453	14 457
$^3F_2$	Γ_3			14 959
	Γ_5			15 133
$^1G_4$	Γ_5	16 611	20 849	20 851
	Γ_3	16 105	21 355	21 356
	Γ_4	16 039	21 421	21 424
	Γ_1	15 951	21 509	21 508
$^3P_2$	Γ_3	37 460	37 460	37 455

[a] From ref 11.

The emission spectrum of $Cs_2NaTmCl_6$ between 37 500 and 15 600 cm^{-1} under 204.2 nm (48 956 cm^{-1}) excitation is shown in Figure 1. These transitions originate from the $^3P_2$ (Γ_3) initial level, observed at 37 460 ± 5 cm^{-1} in the 10 K absorption spectrum of $Cs_2NaTmCl_6$,[11] terminating upon lower energy crystal field levels. The rationale for these assignments is based upon the following: (i) the spectra are virtually identical with those excited by 199.8 nm (50 034 cm^{-1}), 217.8 nm (45 899 cm^{-1}), and 266 nm (37 583 cm^{-1}) radiation; (ii) the spectra are vibronic in nature, as expected for a cubic Tm^{3+} site, and the derived vibrational energies are in agreement with previous studies of this system;[6] (iii) the derived electronic energies match those previously derived from absorption studies[6,11] (Table 2); and (iv) the gap between $^3P_2$ Γ_3 and the next lowest energy level $^3P_1$ Γ_4 is 1578 cm^{-1}, being spanned by six vibrational quanta, so that efficient luminescence is expected to occur from $^3P_2$ Γ_3 in the absence of cross-relaxation deactivation. Since the next highest crystal field level of $^3P_2$ is Γ_5, at 393 cm^{-1} above the luminescent Γ_3 level, no hot electronic spectral features are observed from this level at 10 K.

Mechanism of Excitation of $TmCl_6^{3-}$. The emission spectrum is rather different under 223.1 nm (44 809 cm^{-1}) excitation, with more intense, sharp zero phonon lines at the energies expected for the Tm^{3+} transitions to lower term multiplets. Evidently, the $^3P_2$ emission occurs from a noncentrosymmetric defect site in this case. No $^3P_2$ emission is observed under 273.9 nm (36 499 cm^{-1}) excitation, since this energy is 950 cm^{-1} lower than that of $^3P_2$ Γ_3, and no $TmCl_6^{3-}$ absorption band exists in this region. Under 245.9 nm (40 655 cm^{-1}) and 239.5 nm (41 471 cm^{-1}) excitation, besides the Tm^{3+} emission, additional bands are clearly observed due to fd → f^2 emission transitions of Pr^{3+} at a cubic site, as well as very weak features due to the strongest emission from intraconfigurational f^2 transitions originating from $^3P_0$.

To summarize the above experiments, 10 K emission from the $^3P_2$ level of $TmCl_6^{3-}$ is observed for laser excitation energies between 50 034 and 45 899 cm^{-1}, and also under direct excitation into the $^3P_2$ vibronic sideband using 37 583 cm^{-1} laser radiation. Since there are no further f^{12} Tm^{3+} energy levels above the $^3P_2$ vibronic cutoff (38 300 cm^{-1}) up to the $^1S_0$ level (calculated to be above 71 000 cm^{-1}), or even up to the $f^{11}d$ levels (estimated to be above 55 000 cm^{-1}), the direct population of a Tm^{3+} crystal field level by the laser radiation used in our experiments is not possible. Cresswell et al.[8] have investigated the room-temperature $^3F_4$, $^1D_2$, and $^1G_4$ excitation spectrum of Tm^{3+} diluted into Cs_2NaYCl_6. Two broad ultraviolet bands were observed: (i) between 51 800 and 44 250 cm^{-1}, assigned to a $TmCl_6^{3-}$ charge-transfer transition;[8] (ii) between 31 000 and 38 900 cm^{-1}, which corresponds to unresolved f^{12} transitions to terminal $^3P_2$ and $^1I_6$ levels. Blasse[15] has cited previous work where the first charge-transfer band of $TmCl_6^{3-}$ has been located in the absorption spectrum at ca. 46 800 cm^{-1}. This charge-transfer band is weak (the corresponding feature in $YbCl_6^{3-}$ has $\epsilon_{max} = 160$ mol^{-1} dm^3 cm^{-1})[15] and presumably corresponds to the ligand t_{1g} → metal a_{2u} transition. At 10 K, the hot bands at the low energy side of the charge-transfer transition are expected to disappear. Thus, our 223 nm (44 809 cm^{-1}) laser excitation was not absorbed by $TmCl_6^{3-}$, but by a defect site, and produced trap emission. Our other, higher energy, laser excitation lines were directly into the charge-transfer band. Although the 245.9 nm (40 655 cm^{-1}) and 239.5 nm (41 471 cm^{-1}) excitation lines fall into a band gap, absorption occurred by Pr^{3+} impurities, which have strong, electric dipole allowed, f^2 → fd absorption bands in this region.[16] In fact, the lowest fd level of Pr^{3+} diluted into $Cs_2NaTmCl_6$ is at 38 723 cm^{-1},[16] which is just above the upper limit of the Tm^{3+} $^3P_2$ vibronic structure in the absorption spectrum, so that *in addition* to fd → f^2 emission of Pr^{3+}, nonresonant energy transfer is expected to occur from Pr^{3+} to Tm^{3+}.

van Pieterson et al.[17] have noted that emission from charge-transfer states of lanthanide ions has only been observed for Ce^{4+} and Yb^{3+}. The accepted model for the quenching of this broad-band emission[15,17] is that the parabola of the charge-transfer state, in the configuration coordinate diagram, is considerably shifted along the metal−ligand stretching coordinate, relative to the (very similar) positions of the f-electron states. Nonradiative decay from the charge-transfer state is then facilitated by the parabola crossover with the f-electron parabolas.

Energy Level Assignments. The terminal levels of the $^3P_2$ transitions are readily assigned, from the known energy level scheme,[11] to crystal field levels of the $^3H_6$ ground-state term, and other terms up to those of $^1G_4$. The locations of these crystal field levels are marked in Figure 1. Under the excitation conditions employed, luminescence is not observed from lower levels of Tm^{3+}, except for $^3H_4$. The transition from $^3P_2$ to $^3F_2$ is very weak, and it is not discussed further. The derived energy levels are in agreement with the more accurate locations from the absorption spectrum of the $Cs_2NaTmCl_6$ crystal (Table 2). Two transitions are of particular interest and are described in more detail.

$^3P_2$ → $^3H_4$ Transition of $Cs_2NaTmCl_6$. Figure 1d shows the $^3P_2$ Γ_3 → $^3H_4$ transition, between 25 000 and 24 000 cm^{-1}. The analysis of the vibronic structure (Table 3) is consistent with the assignment of terminal $^3H_4$ Γ_5, Γ_3, Γ_4, and Γ_1 crystal field levels from the absorption spectrum of $Cs_2NaTmCl_6$.[11] However, some strong features then remain unassigned—in particular, the

TABLE 3: Assignment of the 10 K $^3P_2 \rightarrow {}^3H_4$ Emission Spectrum of $Cs_2NaTmCl_6$

line, Figure 1d	energy (cm^{-1})	terminal $^3H_4$ state and derived vibrational energy[a]
1	24 926 vw	Γ_5
2	24 904 w	defect origin, Γ_5
3	24 894 vw	$\Gamma_5 + ZB\ ac\ (32)$
4	24 882 w	$\Gamma_5 + S_5\ (44)$
5	24 869 vw	$\Gamma_5 + S_9\ (57)$
6	24 840 m	$\Gamma_5 + S_{10}\ (86)$
7	24 820 m	$\Gamma_3 + ZB\ ac\ (37)$
8	24 810 m	$\Gamma_5 + S_7\ (116)$
		$\Gamma_3 + S_5\ (47)$
9	24 770 m	$\Gamma_3 + S_{10}\ (87)$
10	24 746 m	$\Gamma_5 + S_8\ (180)$
		$\Gamma_3 + S_7\ (111)$
11	24 733 w, sh	$\Gamma_3 + S_7\ (124)$
		$\Gamma_{4a} + ZB\ ac\ (35)$
12	24 726 w, sh	$\Gamma_{4a} + S_5\ (42)$
13	24 713 vw, sh	$\Gamma_{4a} + S_9\ (55)$
14	24 682 s	$\Gamma_5 + S_6\ (244)$
		$\Gamma_{4a} + S_{10}\ (86)$
15	24 662 m	$\Gamma_5 + S_6\ (264)$
		$\Gamma_{4a} + S_7\ (106)$
16	24 636 m	$\Gamma_5 + S_6\ (290)$
17	24 611 w, sh	$\Gamma_3 + S_6\ (246)$
18	24 599 m	$\Gamma_3 + S_6\ (258)$
19	24 572 bw	$\Gamma_3 + S_6\ (285)$
20	24 565 vw	$\Gamma_{4b} + S_9\ (55)$
21	24 538 m	$\Gamma_{4b} + S_{10}\ (82)$
		$\Gamma_1 + S_5\ (45)$
22	24 493 bm	$\Gamma_1 + S_{10}\ (90)$
23	24 472 w, sh	$\Gamma_1 + S_7\ (109)$
24	24 458 w, sh	$\Gamma_1 + S_7\ (125)$
25	24 337 w, sh	$\Gamma_1 + S_6\ (244)$
26	24 323 w	$\Gamma_1 + S_6\ (258)$
27	24 295 w	$\Gamma_1 + S_6\ (286)$

[a] The initial state is $^3P_2\ \Gamma_3$ in all cases. Refer to Table 1 for the description of vibrational modes. The labeling of vibrations is simplified under the unit cell group model, but the actual spectral features involve contributions from different points in **k** space.

strongest band at 24 682 cm^{-1} (line 14). Part of the intensity of this band could arise from $\Gamma_1 \rightarrow \Gamma_3 + \nu_3$, S_6 (244), but then the higher energy component of S_6 near 259 cm^{-1} would then be more intense than this band, as in all other transitions comprising S_6. This is not observed to be so. Alternatively, this band, and several others, can be assigned to a further electronic transition with the electronic origin located at 24 768 cm^{-1}. The derived energy of the $^3H_4$ terminal state is then 12 692 cm^{-1}.

These results for an "additional" $^3H_4$ energy level may be rationalized in a manner similar to the observation of two aΓ_5 crystal field levels in the electronic ground state, $^3H_6$. In the latter case, it has been shown[18] that a temperature-dependent electron−phonon coupling occurs between the $\Gamma_1 + \nu_5$ vibronic level and the aΓ_5 electronic level, to produce two electron−phonon coupled states at low temperature. For the $^3H_4$ case, we suggest that the coupling occurs between $\Gamma_5 + \nu_2 = 12\,538 + 237 = 12\,775$ cm^{-1} and Γ_4. The $^3H_4\ \Gamma_4$ level is calculated to be near 12 747 cm^{-1},[10,11] which constitutes a large error of 93 cm^{-1} from the previously assigned experimental value of 12 840 cm^{-1}. Taking the values 12 775 and 12 747 cm^{-1} for the unperturbed state energies, and the values 12 840 and 12 692 cm^{-1} for the perturbed state energies, an approximate calculation of the matrix element W of the electron−phonon coupling Hamiltonian from the equation

$$\begin{vmatrix} E(\Gamma_4) - E) & W \\ W & E(\Gamma_5 + \nu_2) - E \end{vmatrix} = 0 \qquad (1)$$

TABLE 4: Assignment of the 10 K $^3P_2 \rightarrow {}^3F_3$ Emission Spectrum of $Cs_2NaTmCl_6$

line, Figure 1e	energy (cm^{-1})	terminal $^3F_3$ state and derived vibrational energy[a]
1	23 034 m	Γ_4
2	23 007 m	Γ_5
3	23 001 w, sh	$\Gamma_4 + ZB\ ac\ (33)$
4	22 995 ms	$\Gamma_4 + S_5\ (39)$
5	22 978 m	$\Gamma_4 + S_9\ (56)$
		$\Gamma_5 + ZB\ ac\ (29)$
6	22 951 s	$\Gamma_4 + S_{10}\ (83)$
		$\Gamma_5 + S_9\ (56)$
7	22 922 m	$\Gamma_5 + S_{10}\ (85)$
8	22 918 m, sh	$\Gamma_4 + S_7\ (116)$
9	22 908 vw	$\Gamma_2 + S_{10}\ (85)$
10	22 898 w	$\Gamma_5 + S_7\ (109)$
11	22 881 w, sh	$\Gamma_5 + S_7\ (126)$
		$\Gamma_2 + S_7\ (112)$
12	22 852 vw, sh	$\Gamma_4 + S_8\ (182)$
13	22 827 vw	$\Gamma_5 + S_8\ (180)$
14	22 791 vw, sh	$\Gamma_4 + S_6\ (243)$
15	22 780 w	$\Gamma_4 + S_6\ (254)$
16	22 763 bw	$\Gamma_5 + S_6\ (244)$
18	22 751 w	$\Gamma_5 + S_6\ (256)$
		$\Gamma_4 + S_6\ (285)$
		$\Gamma_2 + S_6\ (241)$
19	22 736 w	$\Gamma_2 + S_6\ (257)$
20	22 715 vw, b	$\Gamma_5 + S_6\ (286)$
		$\Gamma_2 + S_6\ (285)$
21	22 666 vw	$\Gamma_4 + S_{10} + S_1\ (285)$

[a] The initial state is $^3P_2\ \Gamma_3$ in all cases. Refer to Table 1 for the description of vibrational modes, and to the footnote in Table 3.

gives the value $W = 73 \pm 5$ cm^{-1}. This is greater than that found in the $^3H_6$ ground state, 20 cm^{-1}. It is noted that although the energies of $\Gamma_3 + \nu_2 = 12607 + 237 = 12834$ cm^{-1}, and the Γ_4 level at 12840 cm^{-1} are similar, no interaction is expected to occur in that case from symmetry considerations.

$^3P_2 \rightarrow {}^3F_3$ Transition of $Cs_2NaTmCl_6$. The $^3F_3$ crystal field levels Γ_4 and Γ_5 have been assigned at 14431 and 14457 cm^{-1} from the absorption spectrum of $Cs_2NaTmCl_6$. A firm assignment for the remaining level, Γ_2, could not be made. Despite the fact that Γ_2 is *calculated* to be the lowest $^3F_3$ crystal field level,[11] it is certain that Γ_4 is the lowest level, since low temperature emission is observed from $^3F_3\Gamma_4$ under suitable conditions.[6] The assignment of the $^3P_2 \rightarrow {}^3F_3$ emission transition enables a tentative assignment to be made for the $\Gamma_3 \rightarrow \Gamma_2$ electronic origin at 22993 cm^{-1} (Table 4), so that the Γ_2 level is inferred to be at 14467 cm^{-1}.

Quantum Cutting in $Cs_2LiTmCl_6$. The vibrational behavior of $Cs_2LiTmCl_6$ differs from that of $Cs_2NaTmCl_6$, and the energies and assignments of vibronic structure in the electronic spectra are included in Table 1. We have made a preliminary investigation of the emission of $Cs_2LiTmCl_6$ excited by ultraviolet laser radiation, and both the occurrence of emission solely from $^3P_2$, and the derived f^{12} energy levels, are generally similar to the case of $Cs_2NaTmCl_6$. The 199.8 nm (50034 cm^{-1}) excited 10 K emission spectrum of $Cs_2LiYCl_6:Tm^{3+}$ exhibits considerably more transitions, with emission occurring from the $^3P_2$, $^1I_6$, $^1D_2$ and $^1G_4$ terms in the region above 20000 cm^{-1}. Evidently, ion-ion cross-relaxation processes operate in the neat $Cs_2LiTmCl_6$ crystal to depopulate $^1I_6$, $^1D_2$ and $^1G_4$, and the mechanisms of the latter two processes have previously been described in detail for $Cs_2NaTmCl_6$.[10,19−21] The lowest $^1I_6$ crystal field level, Γ_3, can be depopulated by a resonant cross-relaxation energy transfer mechanism:

$$^1I_6\ \Gamma_3\ (\text{site 1}) + {}^3H_6\ \Gamma_1(\text{site 2}) \rightarrow {}^1G_4\ \Gamma_1(\text{site 1}) + {}^3H_4\ \Gamma_3(\text{site 2}) \qquad (2)$$

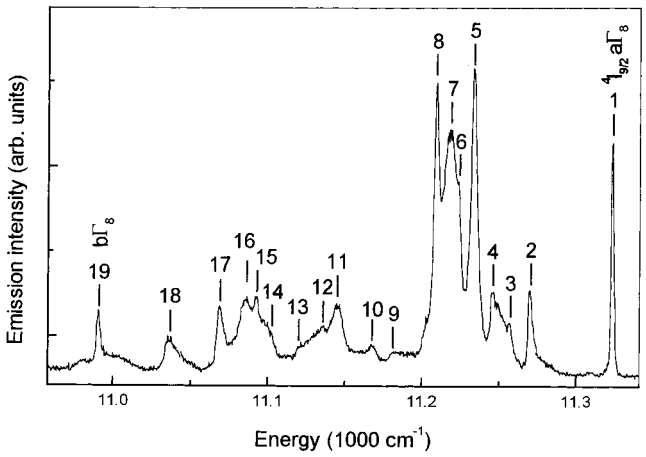

Figure 2. The 476.5 nm excited 10 K luminescence spectrum of $Cs_2LiTmCl_6$, containing trace amounts of Nd^{3+}, between 11 350 and 10 950 cm^{-1}. Refer to Table 5 for band assignments.

TABLE 5: Assignment of the $^4F_{3/2}$ $\Gamma_8 \rightarrow {}^4I_{9/2}$ Luminescence Transition of $Cs_2LiTmCl_6$:Nd^{3+}

line, Figure 2	energy (cm^{-1})	terminal $^4I_{9/2}$ state and derived vibrational energy[a]
1	11 323 s	$a\Gamma_8$
2	11 270 m	$a\Gamma_8 + S_5$ (53)
3	11 257 w	$a\Gamma_8 + S_9$ (66)
4	11 247 bw	$a\Gamma_8 + S_{10}$ (76)
5	11 233 s	$a\Gamma_8 + S_{10}$ (90)
6	11 224 sh	$a\Gamma_8 + S_7$ (99)
7	11 218 bs	$a\Gamma_8 + S_7$ (105)
8	11 209 s	$a\Gamma_8 + S_7$ (114)
9	11 181 vw	$\Gamma_6 + S_5$ (53)
10	11 167 w	$\Gamma_6 + S_9$ (67)
11	11 145 w	$\Gamma_6 + S_{10}$ (89)
12	11 135 mw	$\Gamma_6 + S_7$ (99)
13	11 120 w	$\Gamma_6 + S_7$ (114)
14	11 101 sh	$a\Gamma_8 + S_8$ (222)
15	11 093 mw	$a\Gamma_8 + S_6$ (230)
16	11 087 mw	$a\Gamma_8 + S_6$ (236)
17	11 069 mw	$a\Gamma_8 + S_6$ (254)
18	11 036 w	$a\Gamma_8 + S_6$ (287)
19	10 991 w	$b\Gamma_8$

[a] The initial state is $^4F_{3/2}$ Γ_8 (11 323 cm^{-1}) in all cases. The $^4I_{9/2}$ electronic energies are (in cm^{-1}) 0 ($a\Gamma_8$), 89 (Γ_6), and 332 ($b\Gamma_8$). The vibrational modes are described in Table 1, but refer to the footnote in Table 3.

The spectrum of *neat* $Cs_2LiTmCl_6$ under 476.5 nm argon ion laser excitation, which populates $^1G_4$ vibronic levels, also shows the cross-relaxation quenching of $^1G_4$ emission. No visible emission is observed, and the highest energy luminescence corresponds to $^3H_4 \rightarrow {}^3H_6$, between 12 534 and 11 907 cm^{-1}. To lower energy, a further group of bands is observed (Figure 2) which is assigned to the $^4F_{3/2}$ $\Gamma_8 \rightarrow {}^4I_{9/2}$ transition of trace Nd^{3+} impurity (Table 5). Near-ultraviolet excitation thus produces near-infrared emission either from two Tm^{3+} ions or from one Tm^{3+} and one Nd^{3+} ion. In the latter case, the cross-relaxation is nonresonant, but several mechanisms are possible with donor−acceptor energy mismatches of 15−36 cm^{-1}. The Tm^{3+} ion relaxes from $^1G_4$ to $^3H_5$, while Nd^{3+} transits from $^4I_{9/2}$ to $^4F_{5/2}$ or $^2H_{9/2}$, which then relaxes nonradiatively to $^4F_{3/2}$, Figure 3.

Upconversion to $^3P_2$ in $Cs_2NaTmCl_6$. Figure 4a shows the room-temperature emission spectra of $Cs_2NaGdCl_6$ doped with 10% Tm^{3+}, with excitation into $^1G_4$. Weak emission is observed from $^1G_4$ to lower levels in diluted samples, but this is totally quenched in neat $Cs_2NaTmCl_6$,[6,19] with the highest energy

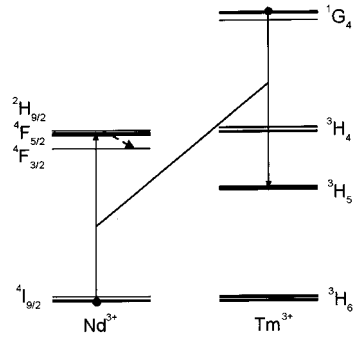

Figure 3. Suggested mechanism of quantum cutting in $Cs_2LiTmCl_6$:Nd^{3+}. Only the relevant energy levels are shown, and initially populated states are circled.

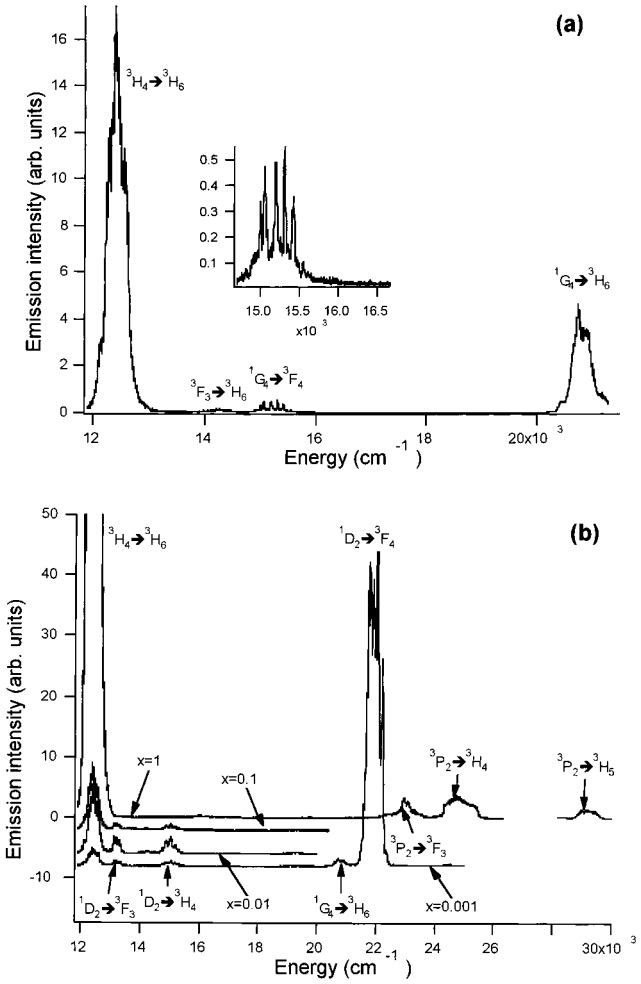

Figure 4. Survey room-temperature emission spectra of (a) $Cs_2NaGd_{0.9}Tm_{0.1}Cl_6$ under 467.76 nm excitation into $^1G_4$; (b) $Cs_2NaGd_{1-x}Tm_xCl_6$ ($x = 0.001-1$) under 360.97 nm excitation into $^1D_2$. The insert in (a) is the extended $^1G_4 \rightarrow {}^3F_4$ emission region.

emission then resulting from the $^3H_4 \rightarrow {}^3H_6$ transition. No upconverted emission from $^1D_2$ or higher levels is observed. The corresponding survey emission spectra for excitation into $^1D_2$ are shown in Figure 4b, for $Cs_2NaGdCl_6$ doped with 0.1−100% Tm^{3+}. In the diluted samples, emission is observed from $^1D_2$ which terminates upon $^3F_4$, $^3H_5$, $^3H_4$, $^3F_3$, and $^3F_2$, with the most intense transition being $^1D_2 \rightarrow {}^3F_4$. The $^3H_4 \rightarrow {}^3H_6$ transition is also observed near 800 nm. By increasing Tm^{3+} concentration, the intensity of emission from $^3H_4$ increases relative to that from $^1D_2$. In neat $Cs_2NaTmCl_6$, however, emission from $^1D_2$ is quenched, and new transitions appear

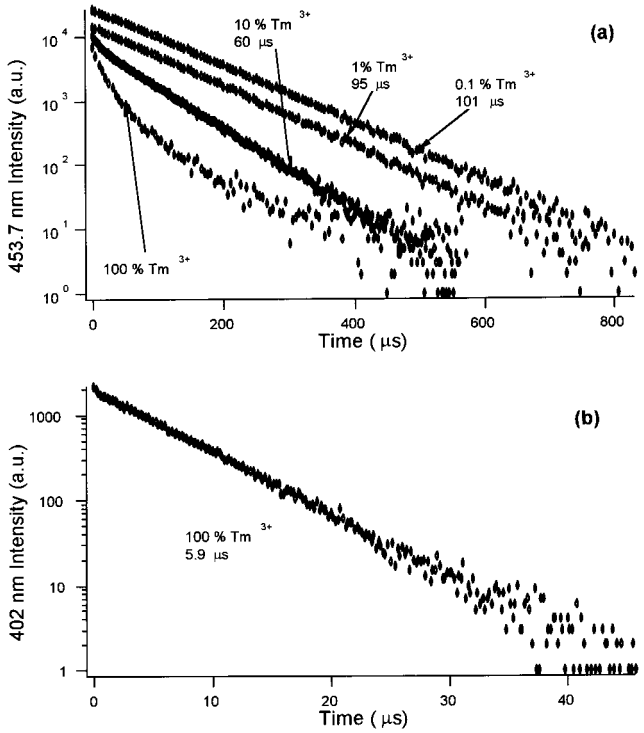

Figure 5. Room-temperature luminescence decay profiles of Tm^{3+} doped into $Cs_2NaGdCl_6$ for (a) $^1D_2$ emission at 453.7 nm; (b) $^3P_2$ emission at 402.0 nm. The fitted natural lifetimes are marked, but emission from $^1D_2$ in *neat* $Cs_2NaTmCl_6$ is not mono- or biexponential.

which originate from $^3P_2$. The energies of these transitions are consistent with those in Figure 1, but also emission from the thermally populated $^3P_2$ Γ_5 level, at 393 cm^{-1} above $^3P_2$ Γ_3, is clearly indicated. The luminescence decay from $^1D_2$ becomes markedly non-monoexponential in the neat sample, and cannot even be fitted by two exponential functions. The emission from $^3P_2$ does not show a detectable rise time (Figure 5), which is indicative of excited-state absorption (ESA) rather than energy-transfer upconversion. It is clear that, besides upconversion, *other* depopulation processes operate for $^1D_2$ in neat $Cs_2NaTmCl_6$, such as the cross-relaxation energy transfer:

$$^1D_2\,(\text{site 1}) + {}^3H_6\,(\text{site 2}) \rightarrow {}^3H_4\,(\text{site 1}) + {}^3F_2\,(\text{site 2}) \quad (3)$$

where $^3F_2$ also decays nonradiatively to $^3H_4$.

The observation of $^3P_2$ upconversion was surprising to us, but its mechanism requires further experiments for elucidation, furthermore since the $Cs_2NaGdCl_6$ host employed is not fully transparent below the energy of the $^3P_2$ Tm^{3+} level.[22]

Conclusions

The emission spectra of Tm^{3+} in elpasolite lattices are rich and show marked changes with increasing concentration of Tm^{3+} in the crystal. For the first time that we are aware of, firm assignments have been given for emission excited by ultraviolet laser radiation, at low temperatures, from the $^3P_2$ state, located near 37 500 cm^{-1}. The most intense transitions are to the terminal $^3H_6$ and $^3F_4$ term manifolds, and are almost entirely vibronic in character. The interpretation of the $^3P_2 \rightarrow {}^3H_4$ emission transition reveals electron−phonon coupling phenomena which provide a clear explanation of the apparently enormous deviation between the experimental and calculated energy of the $^3H_4$ Γ_4 level. A new assignment has also been suggested for $^3F_3$ Γ_2. Conversion of blue to infrared radiation in $Cs_2LiTmCl_6$ and upconversion from $^1D_2$ to $^3P_2$ in $Cs_2NaTmCl_6$ have been shown to occur. While the mechanism for the former process is clear, that for the latter requires further investigation.

Acknowledgment. P.A.T. acknowledges funding from CERG Grant CityU 1067/99P.

References and Notes

(1) Wegh, R. T.; Meijerink, A.; Lamminmäki, R.-J.; Hölsä, J. *J. Lumin.* **2000**, *87*, 1002.
(2) Tanner, P. A.; Chua, M.; Kwok, W. M.; Phillips, D. L. *Phys. Rev.* **1999**, *B60*, 13902.
(3) Dieke, G. H. *Spectra and Energy Levels of Rare Earth Ions in Crystals*; Interscience: New York, 1968.
(4) Hölsä, J.; Lamminmäki, R. J.; Fidancev, E. A.; Lemaitreblaise, M.; Porcher, P. *J. Phys. Condensed Matter* **1995**, *7*, 5127.
(5) Wyss, C. P.; Kehrli, M.; Huber, Th.; Morris, P. J.; Lüthy, W.; Weber, H. P.; Zagumennyi, A. I.; Zavartsev, Yu. D.; Studenikin, P. A.; Shsherbakov, I. A.; Zerrouk, A. F. *J. Lumin.* **1999**, *82*, 137.
(6) (a) Tanner, P. A. *Mol. Phys.* **1984**, *53*, 813, 835. (b) Tanner, P. A. *Mol. Phys.* **1985**, *54*, 883.
(7) Joubert, M. F.; Guy, S.; Cuerq, S.; Tanner, P. A. *J. Lumin.* **1997**, *75*, 287.
(8) Cresswell, P. J.; Robbins, D. J.; Thomson, A. J. *J. Lumin.* **1978**, *17*, 311.
(9) Kirk, A. D.; Furer, N.; Güdel, H. U. *J. Lumin.* **1996**, *68*, 77.
(10) Foster, D. R.; Reid, M. F.; Richardson, F. S. *J. Chem. Phys.* **1985**, *83*, 3225.
(11) Tanner, P. A.; Kumar, V. V. R. K.; Jayasankar, C. K.; Reid, M. F. *J. Alloys Compd.* **1994**, *215*, 349.
(12) Morss, L. R.; Siegel, M.; Stinger, L.; Edelstein, N. *Inorg. Chem.* **1970**, *9*, 1771.
(13) Meyer, G.; Ax, P. *Mater. Res. Bull.* **1982**, *17*, 1447.
(14) Lentz, A. *J. Phys. Chem. Solids* **1974**, *35*, 827.
(15) Blasse, G. *Struct. Bonding* **1976**, *26*, 43.
(16) Tanner, P. A.; Mak, C. S. K.; Faucher, M. D. *Chem. Phys. Lett.* **2001**, *343*, 309.
(17) van Pieterson, L.; Heeroma, M.; de Heer, E.; Meijerink, A. *J. Lumin.* **2000**, *91*, 177.
(18) Tanner, P. A.; Xia, S.; Liu, Y. L.; Ma, Y. *Phys. Rev.* **1997**, *B55*, 12182.
(19) Tanner, P. A.; Chua, M.; Reid, M. F. *J. Alloys Compd.* **1995**, *225*, 20.
(20) O'Connor, R.; Mahiou, R.; Martinant, D.; Fournier, M. T. *J. Alloys Compd.* **1995**, *225*, 107.
(21) Kirk, A. D.; Furer, N.; Güdel, H. U. *J. Lumin.* **1996**, *68*, 77.
(22) de Vries, A. J.; Blasse, G. *J. Chem. Phys.* **1988**, *88*, 7312.